

Diagonal Hierarchical Consistency Learning for Semi-supervised Medical Image Segmentation

Heejoon Koo[†]

Abstract—Medical image segmentation, which is essential for many clinical applications, has achieved almost human-level performance via data-driven deep learning technologies. Nevertheless, its performance is predicated upon the costly process of manually annotating a vast amount of medical images. To this end, we propose a novel framework for robust semi-supervised medical image segmentation using diagonal hierarchical consistency learning (DiHC-Net). First, it is composed of multiple sub-models with identical multi-scale architecture but with distinct sub-layers, such as up-sampling and normalisation layers. Second, with mutual consistency, a novel consistency regularisation is enforced between one model’s intermediate and final prediction and soft pseudo labels from other models in a diagonal hierarchical fashion. A series of experiments verifies the efficacy of our simple framework, outperforming all previous approaches on public benchmark dataset on organ and tumour.

Index Terms—Medical Image Segmentation, Semi-supervised Learning, Consistency Regularization, Multi-scale Networks, Entropy Minimization, Uncertainty Estimation

I. INTRODUCTION

Medical image segmentation (MIS) involves assigning each pixel in an image to a specific class of anatomical structure, such as organs, tissues and tumours. This task provides valuable information for both computer-aided diagnosis (CAD) and computer-assisted surgery (CAS) in intuitive and efficient manner. Recently, deep learning with U-Net-based architectures [1], [2] has significantly improved MIS. Nonetheless, acquiring a large volume of high-quality annotated medical images remains labour-intensive and time-consuming, necessitating medical experts to manually annotate intricate medical images. To address this issue, many studies have endeavoured on semi-supervised learning that uses a small set of labelled data in conjunction with a large set of unlabelled data [3].

Accordingly, semi-supervised medical image segmentation (SSMIS) has undergone significant advancements. After a seminal work by [4], [5] extends it by leveraging deep supervision and hierarchical consistency regularisation. Meanwhile, [6] predicts Signed Distance Maps (SDM) [7] as an auxiliary task in an adversarial manner [8] to produce more realistic predictions. Thereafter, [9] introduces dual task consistency between the SDM regression and segmentation prediction.

Another line of literature [4], [10], [11] introduces uncertainty estimation. Yu et al. [4] introduces uncertainty maps obtained via Monte-Carlo (MC) Dropout [12] to predict with

higher confidence in a teacher-student framework. On the other hand, based on finding [13] that uncertainty can be quantified by a statistical discrepancy from multiple model predictions, [10], [11] design a network with multiple distinct sub-models.

During the advancement of SSMIS, AI research community has delved into normalisation layers. Instance normalisation [14] is developed for style transfer, while group normalisation [15] has shown great stability on relatively small batch sizes. Albeit these findings, the utilisation of various normalisation layers in SSMIS still remains under-investigated.

Motivated by recent advancements, we introduce a novel SSMIS framework under the assumption that a network, composed of diversified sub-models, can first fully learn from the scarce labelled data then collaborate by minimising disparities in predictions on uncertain regions yielded from both labelled and unlabelled data. Therefore, the main contributions of this paper is threefold. First, we design the network to be comprised of three identical multi-scale V-Nets [2] with distinct sub-layers, such as up-sampling and normalisation layers to increase intra-model diversity. Second, it is optimised via deep supervision on labelled data and our proposed diagonal hierarchical consistency learning as well as mutual consistency learning [10] on both labelled and unlabelled data. Finally, this simple yet effective framework demonstrates its superiority by surpassing existing baselines on publicly available dataset. on Left Atrium (LA) [16] and Brain Tumor Segmentation (BraTS) 2019 dataset [17].

II. METHODOLOGIES

A. Task Formulation

In SSMIS, a set of training data has N labelled data and M unlabelled data, where $N \ll M$. Then, the small set of labelled data is denoted as $\mathcal{D}_L = \{x_i^l, y_i\}_{i=1}^N$ and remaining set of unlabelled data as $\mathcal{D}_U = \{x_i^u\}_{i=1}^M$, where x_i^l and x_i^u denotes the input images and y_i the corresponding segmentation masks. The objective is to train a model f_θ , parameterised with θ , using the full data $\mathcal{D} = \mathcal{D}_L \cup \mathcal{D}_U$ to perform pixel-wise classification correctly.

B. Diversifying Multi-scale Sub-models and Deep Supervision

Following the previous works [10], [11], we employ a network with three sub-models having the identical architecture but with a variance in their sub-layers. Specifically, we use group normalisation [15] and linear interpolation for the first sub-model’s normalisation and up-sampling, respectively. The second sub-model configures with transposed convolution and

[†]Department of Electronic and Electrical Engineering, University College London, London, United Kindom. Email: heejoon.koo.17@alumni.ucl.ac.uk

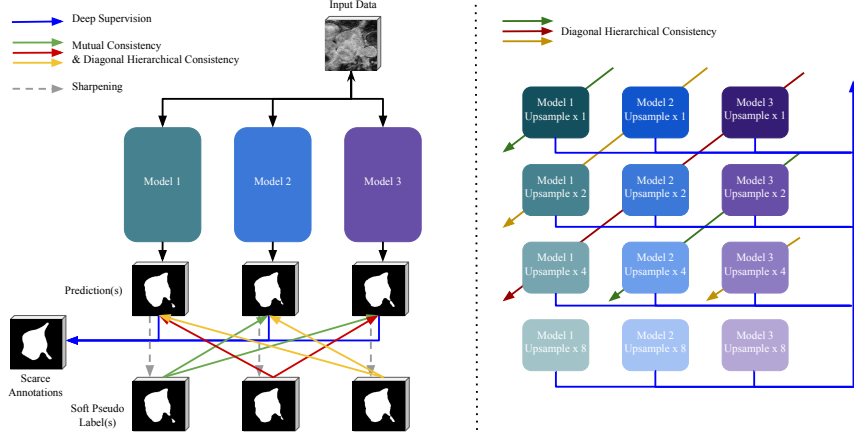


Fig. 1. An Overview of Our Proposed Framework, DiHC-Net. The left provides a high-level conceptualisation of the proposed framework, whilst the right presents a visualisation on both deep-supervision and diagonal hierarchical consistency.

batch normalisation [18] and the third model adopts nearest interpolation and instance normalisation [14].

Also, we extend our sub-models to have multi-scale architecture to produce intermediate representations from each block in their decoding stage. On the labelled data, the network learns scarce supervisory signal effectively by minimising the differences between up-sampled intermediate predictions and ground truths in each sub-models. This supervised segmentation loss is mathematically formulated as:

$$\mathcal{L}_{sup} = \sum_{m=1}^M \sum_{s=1}^S \mathcal{L}_{dice}(f_m^s(x_i^l), y_i), \quad (1)$$

where \mathcal{L}_{dice} represent dice loss, $f_m^s(\cdot)$ denotes the predicted results from at scale s of m -th model. Both s and m are integers, ranging from 1 to 3 and 4, respectively.

C. Diagonal Hierarchical Consistency Learning

Boosting diversity amongst sub-models leads to increased inconsistent predictions especially in challenging regions. These uncertainties can be mitigated effectively by employing pseudo labels to minimise entropy across the models. Previous studies [10], [11] minimise them through the enforcement of a mutual consistency loss. However, they do not consider intermediate outputs. Addressing this gap, we introduce our novel diagonal hierarchical consistency loss. We use two consistency losses to both labelled and unlabelled data.

First, we enforce mutual consistency between the soft pseudo labels converted from one sub-model's final prediction and others' final predictions. The sharpening function [19] is utilised to acquire the soft pseudo label as follows:

$$S^{M_n} = \text{sharpening}(p^{M_n}), \quad (2)$$

$$\text{where sharpening} = \frac{p^{1/T}}{p^{1/T} + (1-p)^{(1/T)}}.$$

Here, S and p represent the pseudo label and prediction, respectively, while M_n denotes the n -th model. The hyper-parameter T serves to control entropy; a lower T promotes

low-entropy predictions. Then, with α_k as coefficient for the k -th block at the reverse decoding order, formulation of the mutual consistency loss using mean squared error (MSE) is:

$$\mathcal{L}_{mc} = \sum_{i,j=1 \& i \neq j}^n \alpha_1 \text{MSE}(S_i^{M_i}, p_j^{M_j}). \quad (3)$$

Next, our novel diagonal hierarchical consistency minimises the difference between one sub-model's pseudo labels converted from its final representation and others' intermediate and last representations. We design it to be computationally efficient and not redundant, enabling the mutual regularisation of predictions across all models.

Let the coordinate of representation as (m -th model, s -th representation). Then, the representation from the last decoding block of the first model is (1, 1). Similarly, the representation from the first decoding block of the third model is (3, 4). Self-constraint is enforced between the pseudo label and the first decoder block from the same model if following our consistency, but not conducted due to empirical harmful effects. Thus, the regarding loss is:

$$\begin{aligned} \mathcal{L}_{dhc} = & \alpha_2 \text{MSE}(S_1^{M_1}, p_2^{M_3}) + \alpha_3 \text{MSE}(S_1^{M_1}, p_3^{M_2}) \\ & + \alpha_2 \text{MSE}(S_2^{M_2}, p_2^{M_1}) + \alpha_3 \text{MSE}(S_2^{M_2}, p_3^{M_3}) \\ & + \alpha_2 \text{MSE}(S_3^{M_3}, p_2^{M_2}) + \alpha_3 \text{MSE}(S_3^{M_3}, p_3^{M_1}). \end{aligned} \quad (4)$$

Therefore, the network is optimised via a weighted sum of supervised loss \mathcal{L}_{sup} and consistency loss \mathcal{L}_{cst} .

$$\begin{aligned} \mathcal{L}_{total} = & \lambda_{sup} \mathcal{L}_{sup} + \lambda_{cst} \mathcal{L}_{cst}, \\ \text{where } \mathcal{L}_{cst} = & \mathcal{L}_{mc} + \mathcal{L}_{dhc}, \end{aligned} \quad (5)$$

where λ_{sup} denotes a hyper-parameter for the supervised loss and λ_{cst} is the coefficient for the consistency loss, which is a time-dependent Gaussian warming-up function that balances between two loss terms. It is formalised as $\lambda(t) = 0.1 * \exp(-5(1-t/t_{max}))$ where t and t_{max} are present training step and the maximum step, respectively. It

TABLE I
A QUANTITATIVE PERFORMANCE COMPARISON ON THE LA AND BRA TS DATASET.

Method	% Scans used		LA				BraTS			
	Labelled	Unlabelled	Dice(%) \uparrow	Jaccard(%) \uparrow	ASD(voxel) \downarrow	95HD(voxel) \downarrow	Dice(%) \uparrow	Jaccard(%) \uparrow	ASD(voxel) \downarrow	95HD(voxel) \downarrow
UA-MT [4]	10%	90%	84.25	73.48	3.36	13.84	80.85	70.32	2.57	14.61
SASS [6]			86.81	76.92	3.94	12.54	81.96	70.65	4.92	16.99
DTC [9]			87.51	78.17	2.36	8.23	81.96	71.84	2.43	12.08
MC-Net+ [10]			88.96	80.25	1.86	7.93	82.42	72.44	4.38	13.94
CC-Net [11]			89.82	81.60	1.8	7.03	82.74	72.82	3.02	12.29
Ours (DiHC-Net)			90.42	82.58	1.54	6.52	84.96	75.36	2.57	10.33
UA-MT [4]	20%	80%	88.88	80.21	2.26	7.32	81.57	71.42	2.49	13.98
SASS [6]			89.27	80.82	3.13	8.83	80.79	70.56	4.10	13.80
DTC [9]			89.42	80.98	2.1	7.32	82.78	72.47	2.2	13.43
MC-Net+ [10]			91.07	83.67	1.67	5.84	83.24	73.50	2.55	9.78
CC-Net [11]			91.27	84.02	1.54	5.75	83.30	73.34	2.57	10.44
Ours (DiHC-Net)			91.94	85.13	1.35	5.03	85.47	76.13	2.16	9.31

addresses the potential issue of consistency loss term that may harm the learning in the early stage.

III. EXPERIMENTAL SETTING

A. Dataset

To validate the effectiveness of our approach, we conduct experiments on publicly available LA and BraTS 2019 dataset. They provide total 100 and 335 3D MRI scans and corresponding segmentation masks. As test set annotations are publicly unavailable for LA dataset, the training set is divided into two subsets with 80 scans for training and 20 scans for evaluation. BraTS dataset is originally split into 250 scans for training, 25 scans for validation and the remaining 60 scans for testing.

B. Implementation Details

We follow the previous works [4], [6], [10] by employing the same data pre-processing, data augmentation methods, hyper-parameter and optimisation settings for training. Additionally, we do not use any post-processing module (e.g. non-maximum suppression) for a fair comparison.

Soft pseudo labels are generated using a sharpening function with a fixed temperature T of 0.1. We use three intermediate representations and coefficients for each consistency loss are determined as $\alpha_1 = 1.0$, $\alpha_2 = 0.75$, and $\alpha_3 = 0.5$. We set them to gradually decrease, since intermediate blocks should be softly regularised due to their tendency to produce relatively incomplete outputs. Also, we set λ_{sup} as 1.

We experiment on two settings: training with 10% or 20% labelled data and the remaining unlabelled data. Instead of averaging three outputs, we utilise results from the first model, in line with methods from prior research [10], [11]. We measure performance using four metrics: Dice, Jaccard, ASD (Average Surface Distance) and 95HD (95% Hausdorff Distance). The first two metrics assess the interior segmentation predictions, while the last two assess the contour predictions.

IV. EXPERIMENTAL RESULTS

A. Performance Comparison

Tab. I presents the quantitative results of our proposed method and other strong baselines, including UA-MT [4], SASS [6], DTC [9], MC-Net+ [10] and CC-Net [11]. As shown in Tab. I, our DiHC-Net consistently outperforms all

baselines by a large margin consistently in both training settings across both dataset. Fig. 2 visually highlights the effectiveness and robustness of our approach. Our framework produces more natural contours than shape-constraint methods [6], [9] and is more stable to false negatives on both LA and BraTS 2019 dataset.

This superior performance is achieved by multiple sub-models that first fully learn scarce labelled data then reduce discrepancies in ambiguous and challenging areas from one model’s intermediate and final predictions and other’s pseudo labels by employing a our novel diagonal hierarchical consistency approach in all data.

B. Ablation Studies

TABLE II
ABLATION STUDIES ON THE LA DATASET.

% Scans Used		Designs			Metrics	
Labelled	Unlabelled	IMD	MS	DiHC	Dice(%) \uparrow	ASD(voxel) \downarrow
10%	90%				88.96	1.86
			✓		88.69	1.84
			✓	✓	89.09	1.69
		✓		✓	89.53	2.34
		✓	✓		90.13	2.11
		✓	✓	✓	90.42	1.54
20%	80%				91.07	1.67
			✓		91.11	1.5
			✓	✓	91.38	1.44
		✓		✓	91.1	1.82
		✓	✓		91.72	1.72
		✓	✓	✓	91.94	1.35

We also conduct ablation studies to discern each proposed module’s impact on the overall performance using LA dataset. We present the results to Tab. II. Our design components are abbreviated as: 1) Intra-Model Diversity (IMD), 2) Multi-scale Network (MS), and 3) Diagonal Hierarchical Consistency (DiHC). A baseline without any components is [10].

First, applying IMD does not consistently result in overall performance enhancement, particularly when comparing contour-related metric (ASD). This suggests that merely enhancing the diversity in the configurations of sub-models complicates the convergence process. However, the integration of MS and IMD results in performance improvement, as they fully leverage supervisory signals. Furthermore, integrating DiHC to the framework leads to significant gains across both metrics and training settings, verifying our initial hypothesis.

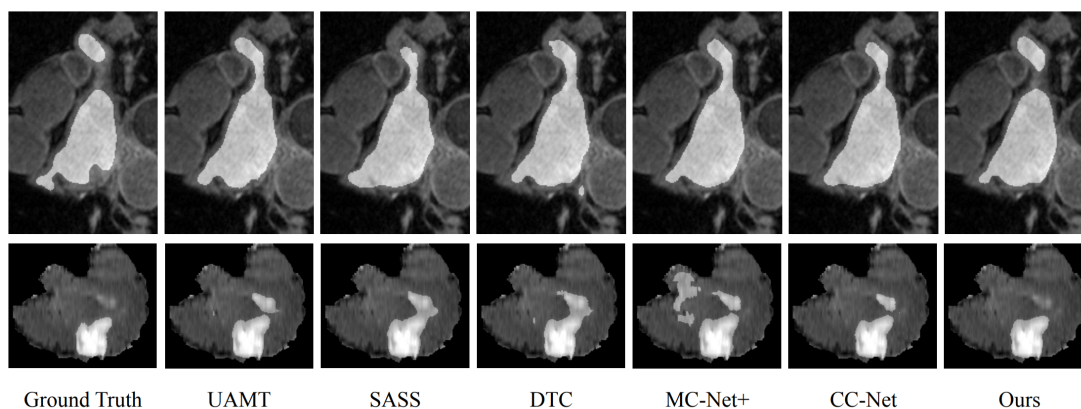


Fig. 2. 2D Visualisation of Ground Truth and Predictions of Our DiHC-Net and Other Baselines on LA and BraTS Dataset. The first row is acquired when trained with 10% labelled data from LA dataset and the second row with 20% labelled data from BraTS dataset.

V. CONCLUSION

In this paper, we present a concise but effective SSMIS framework. Its network is composed of three sub-models with the same multi-scale V-Net but distinct sub-layers. By employing deep supervision, they first learn the limited labelled data. Next, they collaborate by minimising differences on challenging regions by comparing soft pseudo labels from one’s final predictions and others’ intermediate and final outcomes via conventional mutual consistency and our diagonal hierarchical consistency on all data. Experimental results demonstrate the superiority and robustness of our simple DiHC-Net.

REFERENCES

- [1] O. Ronneberger, P. Fischer, and T. Brox, “U-net: Convolutional networks for biomedical image segmentation,” in *Medical Image Computing and Computer-Assisted Intervention–MICCAI 2015: 18th International Conference, Munich, Germany, October 5-9, 2015, Proceedings, Part III 18*. Springer, 2015, pp. 234–241.
- [2] F. Milletari, N. Navab, and S.-A. Ahmadi, “V-net: Fully convolutional neural networks for volumetric medical image segmentation,” in *2016 fourth international conference on 3D vision (3DV)*. Ieee, 2016, pp. 565–571.
- [3] R. Jiao, Y. Zhang, L. Ding, R. Cai, and J. Zhang, “Learning with limited annotations: a survey on deep semi-supervised learning for medical image segmentation,” *arXiv preprint arXiv:2207.14191*, 2022.
- [4] L. Yu, S. Wang, X. Li, C.-W. Fu, and P.-A. Heng, “Uncertainty-aware self-ensembling model for semi-supervised 3d left atrium segmentation,” in *Medical Image Computing and Computer Assisted Intervention–MICCAI 2019: 22nd International Conference, Shenzhen, China, October 13–17, 2019, Proceedings, Part II 22*. Springer, 2019, pp. 605–613.
- [5] S. Li, Z. Zhao, K. Xu, Z. Zeng, and C. Guan, “Hierarchical consistency regularized mean teacher for semi-supervised 3d left atrium segmentation,” in *2021 43rd Annual International Conference of the IEEE Engineering in Medicine & Biology Society (EMBC)*. IEEE, 2021, pp. 3395–3398.
- [6] S. Li, C. Zhang, and X. He, “Shape-aware semi-supervised 3d semantic segmentation for medical images,” in *Medical Image Computing and Computer Assisted Intervention–MICCAI 2020: 23rd International Conference, Lima, Peru, October 4–8, 2020, Proceedings, Part I 23*. Springer, 2020, pp. 552–561.
- [7] J. Ma, Z. Wei, Y. Zhang, Y. Wang, R. Lv, C. Zhu, C. Gaoxiang, J. Liu, C. Peng, L. Wang *et al.*, “How distance transform maps boost segmentation cnns: an empirical study,” in *Medical Imaging with Deep Learning*. PMLR, 2020, pp. 479–492.
- [8] I. Goodfellow, J. Pouget-Abadie, M. Mirza, B. Xu, D. Warde-Farley, S. Ozair, and Y. Bengio, “Generative adversarial networks, 1–9,” *arXiv preprint arXiv:1406.2661*, 2014.
- [9] Y. Zhang and J. Zhang, “Dual-task mutual learning for semi-supervised medical image segmentation,” in *Pattern Recognition and Computer Vision: 4th Chinese Conference, PRCV 2021, Beijing, China, October 29–November 1, 2021, Proceedings, Part III 4*. Springer, 2021, pp. 548–559.
- [10] Y. Wu, Z. Ge, D. Zhang, M. Xu, L. Zhang, Y. Xia, and J. Cai, “Mutual consistency learning for semi-supervised medical image segmentation,” *Medical Image Analysis*, vol. 81, p. 102530, 2022.
- [11] H. Huang, Z. Chen, C. Chen, M. Lu, and Y. Zou, “Complementary consistency semi-supervised learning for 3d left atrial image segmentation,” *Computers in Biology and Medicine*, vol. 165, p. 107368, 2023.
- [12] Y. Gal and Z. Ghahramani, “Dropout as a bayesian approximation: Representing model uncertainty in deep learning,” in *International conference on machine learning*. PMLR, 2016, pp. 1050–1059.
- [13] B. Lakshminarayanan, A. Pritzel, and C. Blundell, “Simple and scalable predictive uncertainty estimation using deep ensembles,” *Advances in neural information processing systems*, vol. 30, 2017.
- [14] D. Ulyanov, A. Vedaldi, and V. Lempitsky, “Instance normalization: The missing ingredient for fast stylization,” *arXiv preprint arXiv:1607.08022*, 2016.
- [15] Y. Wu and K. He, “Group normalization,” in *Proceedings of the European conference on computer vision (ECCV)*, 2018, pp. 3–19.
- [16] Z. Xiong, Q. Xia, Z. Hu, N. Huang, C. Bian, Y. Zheng, S. Vesal, N. Ravikumar, A. Maier, X. Yang *et al.*, “A global benchmark of algorithms for segmenting the left atrium from late gadolinium-enhanced cardiac magnetic resonance imaging,” *Medical image analysis*, vol. 67, p. 101832, 2021.
- [17] B. H. Menze, A. Jakab, S. Bauer, J. Kalpathy-Cramer, K. Farahani, J. Kirby, Y. Burren, N. Porz, J. Slotboom, R. Wiest, L. Lanczi, E. Gerstner, M.-A. Weber, T. Arbel, B. B. Avants, N. Ayache, P. Buendia, D. L. Collins, N. Cordier, J. J. Corso, A. Criminisi, T. Das, H. Delingette, Å. Demiralp, C. R. Durst, M. Dojat, S. Doyle, J. Festa, F. Forbes, E. Geremia, B. Glocker, P. Golland, X. Guo, A. Hamamci, K. M. Iftekharuddin, R. Jena, N. M. John, E. Konukoglu, D. Lashkari, J. A. Mariz, R. Meier, S. Pereira, D. Precup, S. J. Price, T. R. Raviv, S. M. S. Reza, M. Ryan, D. Sarikaya, L. Schwartz, H.-C. Shin, J. Shotton, C. A. Silva, N. Sousa, N. K. Subbanna, G. Szekely, T. J. Taylor, O. M. Thomas, N. J. Tustison, G. Unal, F. Vasseur, M. Wintermark, D. H. Ye, L. Zhao, B. Zhao, D. Zikic, M. Prastawa, M. Reyes, and K. Van Leemput, “The multimodal brain tumor image segmentation benchmark (brats),” *IEEE Transactions on Medical Imaging*, vol. 34, no. 10, pp. 1993–2024, 2015.
- [18] S. Ioffe and C. Szegedy, “Batch normalization: Accelerating deep network training by reducing internal covariate shift,” in *International conference on machine learning*. pmlr, 2015, pp. 448–456.
- [19] Q. Xie, Z. Dai, E. Hovy, T. Luong, and Q. Le, “Unsupervised data augmentation for consistency training,” *Advances in neural information processing systems*, vol. 33, pp. 6256–6268, 2020.